

RESEARCH ARTICLE

View Article Online
View Journal

Cite this: DOI: 10.1039/d5qo00922g

Terpene cyclization catalysis with a functional cavitand: driving selectivity through precise molecular recognition†

Ricard López-Coll ^a and Agustí Lledó ^{*a,b}Received 21st June 2025,
Accepted 14th July 2025
DOI: 10.1039/d5qo00922g
rsc.li/frontiers-organic

A three-walled self-folding cavitand receptor derived from resorcin[4]arene featuring phenol groups near the confined space catalyzes the cyclization reaction of nerol, using HCl as co-catalyst. In contrast to terpene cyclization reactions mediated by other synthetic hosts, the process reported herein is substrate specific, provides very high selectivity towards cyclization products, and delivers limonene—a thermodynamically disfavored product—as the major compound. The observed acceleration, turnover and unique selectivity are rationalized on the basis of precise molecular recognition phenomena, supported by NMR studies and DFT calculations.

Introduction

The application of synthetic host molecules in supramolecular catalysis has emerged in the last decades as a viable and complementary approach to small molecule and biological catalysis.^{1–3} Supramolecular synthetic receptors are well suited to reproduce the confinement, preorganization, and induced fit effects that are central for the emergence of enzymatic catalysis.⁴ While a plethora of synthetic hosts have been reported over the years, coordination cages^{5,6} and self-assembled resorcin[4]arene (R4OH) capsules^{7,8} stand out, thanks in part to their synthetic accessibility (Fig. 1). Advances in this area have allowed surpassing early reports on model reactions of limited impact. One of the most prominent examples is the development of terpene-cyclization catalysis by the (R4OH)₆·(H₂O)₈ capsule (C1), developed by the group of Tiefenbacher,⁹ which allows the preparation of cyclic terpenes of remarkable complexity.¹⁰ However, the control over the reaction selectivity remains challenging in these systems, arguably because of the difficulty in controlling host-substrate complementarity in the large, non-functionalized, and highly symmetrical confined space of C1. In addition, catalysis by C1 favours the most thermodynamically stable cyclization products.¹¹ Recent

efforts to develop less symmetrical assemblies showcase the limitations of the C1-based systems on this front.^{12,13}

Functional self-folding receptors based on R4OH are also promising candidates to develop bioinspired supramolecular catalysis, although only a few examples of catalytic processes have been reported to date using these hosts.^{14–17} In addition to their synthetic complexity, the reduced binding site of R4OH-derived cavitands is an important limitation to uncover new reactivity. Conversely, it is precisely the snug fit offered by these less symmetrical and functionalized confined spaces that offers opportunities for selective reactivity. This is showcased by the epoxide ring opening reaction catalysed by a cavitand with inwardly directed carboxylic acid functionality, developed by the group of Rebek.^{16,17}

As demonstrated by Tiefenbacher, the catalytic performance of C1 rests on a unique proton shuttle mechanism mediated by the convergent phenol units at the vertices of the cage.¹⁸ We hypothesized whether the phenol units in partially bridged self-folding cavitand C2 (Fig. 1) could be exploited to effect terpene cyclization catalysis in a similar manner, eventually providing better control over the reaction outcome on the basis of a binding site of reduced symmetry and better size complementarity to monoterpenes in relation to C1. Partially bridged cavitands like C2 have molecular recognition features that are differentiated from those of their symmetrical counterparts,^{19–21} and have been used as a versatile platform to develop more elaborated functional cavitands.^{14–17,22–32} However, their use as functional supramolecular reactors or catalysts on their own has never been reported, to the best of our knowledge.

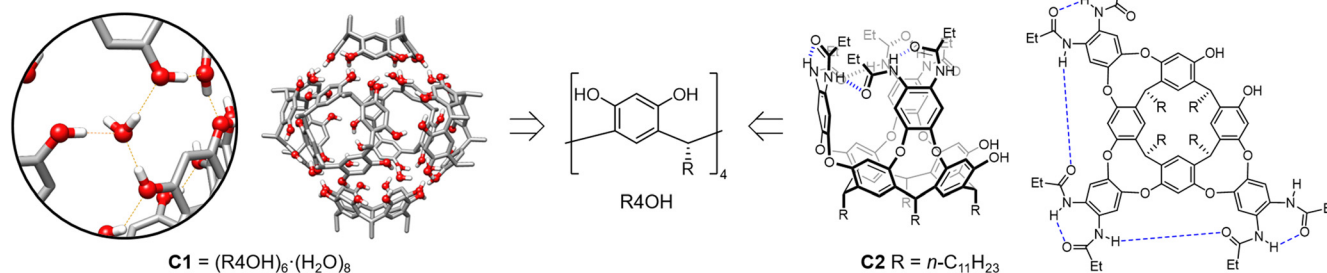
Herein, we disclose the selective cyclization of nerol co-catalysed by receptor C2 and HCl, resulting primarily in the for-

^aInstitut de Química Computacional i Catalisi (IQCC), Universitat de Girona, Maria Aurèlia Capmany 69, 17003 Girona, Spain. E-mail: agusti.lledo@udg.edu

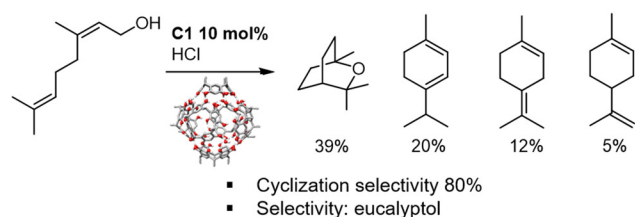
^bInstitute of Chemical Research of Catalonia (ICIQ), The Barcelona Institute of Science and Technology, Av. Països Catalans 16, 43007 Tarragona, Spain

†Electronic supplementary information (ESI) available: Methodology for the terpene cyclization reaction setup and analysis, NMR titration studies, 2D NOESY experiment of TAC2, additional details of the computational studies, and ESI figures. See DOI: <https://doi.org/10.1039/d5qo00922g>



a) Resorcin[4]arene derived hexameric cage **C1** and cavitand **C2**

b) Self-assembled cage catalysis of terpene cyclization



c) This work: cavitand catalysis of terpene cyclization

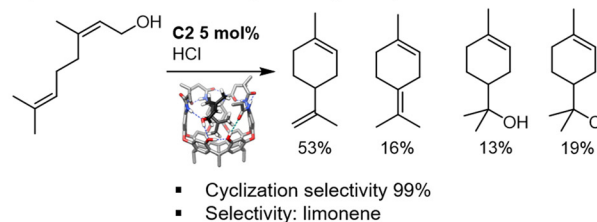


Fig. 1 (a) Structures of the resorcin[4]arene (R4OH) hexameric cage **C1**, highlighting the convergent phenolic groups at the vertices, and schematic structure of the partially bridged self-folding cavitand **C2**. (b) Cyclization of nerol catalysed by **C1** and HCl. (c) Cyclization reaction of nerol catalysed by **C2** and HCl.

mation of limonene and providing complete conversion to cyclic products, a selectivity profile that is not available using **C1** as catalyst (Fig. 1).

Results and discussion

Reaction development and optimization

We started testing our initial hypothesis by subjecting linear monoterpenes to reaction under conditions similar to those reported for capsule-catalysed reactions, using 10 mol% **C2** as catalyst and 10 mol% HCl as co-catalyst in chloroform (Table 1). Reaction monitoring was carried out by GC-FID ana-

lysis, using authentic samples of a variety of available cyclic terpenes as reference (see ESI† for details). When using geraniol (**S1**) or linalool (**S3**) as substrates, moderate conversions were observed, but cyclization products could either not be detected or they were formed in very low yield. Conversely, the cyclization of nerol (**S2**) proceeded to a similar extent in the same time, resulting in almost total selectivity towards cyclic products. Importantly, limonene (**P1**) was identified as the major product in the mixture, alongside lesser amounts of terpinolene (**P2**) and α -terpineol (**P3**). The use of **S4**—differing only from **S2** in the leaving group—resulted in a similar conversion but provided again low yields of cyclic products. Overall, this initial screening positioned nerol (**S2**) as a unique substrate to drive the formation of cyclic products, suggesting a good complementarity for **C2** that is absent in the other substrates.

With these promising results in hand, we next carried out a systematic analysis of the reaction parameters with the objective of increasing substrate conversion rates while keeping the distinct selectivity profile observed. Initial attempts to achieve complete substrate consumption proved challenging, and we proceeded to analyse the reaction progress to identify the cause. Reaction monitoring over time revealed that the reaction progresses rapidly in the first stages and a plateau in conversion and yields is reached in the first 12 hours of reaction (Fig. S3†). We hypothesized that product inhibition was the cause of the observed reaction rate decay, and we proceeded to carry out a number of control experiments (Table 2). Interestingly, none of the observed reaction products (**P1–P3**) resulted in any meaningful inhibition when added at the beginning of the reaction. The addition of water—a by-product of the reaction—did not have a detrimental effect either. Conversely, the addition of a tetra-

Table 1 Initial screening of substrates (**S**) for cyclization reactions catalysed by **C2** and HCl

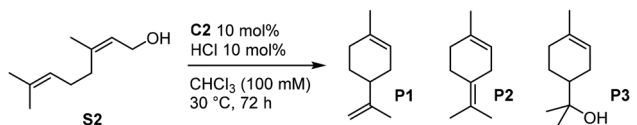
Reaction scheme showing the conversion of substrates **S1**, **S2**, **S3**, and **S4** (where R = prenyl) to products **P1**, **P2**, and **P3** using **C2** (10 mol%), **HCl** (10 mol%), and **CHCl₃** (100 mM) at 30 °C for 72 h.

Entry	S	Conv. [%]	Yield P1 [%]	Yield P2 [%]	Yield P3 [%]	CR [%]
1	S1	19.4 ± 0.4	—	—	—	—
2	S2	23.4 ± 0.7	13.3 ± 0.5	4.5 ± 0.2	4.0 ± 0.1	93
3	S3	25.3 ± 0.7	3.0 ± 0.1	2.4 ± 0.2	—	21
4	S4	19 ± 2	4.3 ± 0.4	2.0 ± 0.3	—	33

Conversion and yields calculated by GC-FID analysis. Cyclic selectivity ratio (CR) obtained by dividing the combined yield of cyclic products by substrate conversion.



Table 2 Control experiments for the cyclization of nerol (**S2**) catalysed by **C2** and HCl (reaction time: 72 h)

								
Entry	C2 [mol%]	HCl [mol%]	Additive	Conv. [%]	Yield P1 [%]	Yield P2 [%]	Yield P3 [%]	CR [%]
1	10	10	P1 10 mol%	24.0 ± 0.8	14.1 ± 0.2 ^a	4.8 ± 0.1	4.2 ± 0.0	96
2	10	10	P2 10 mol%	26 ± 1	16 ± 1	4.6 ± 0.5 ^a	4.7 ± 0.5	95
3	10	10	P3 10 mol%	24.8 ± 0.3	14.3 ± 0.2	4.9 ± 0.0	5.7 ± 0.1 ^a	>99
4	10	10	H ₂ O 10 mol%	29 ± 1	19 ± 1	6.0 ± 0.5	5.0 ± 0.2	>99
5	10	10	Me ₄ N ⁺ AcO ⁻ 20 mol%	0	—	—	—	—
6	10	—	—	0.1 ± 0.3	—	—	—	—
7	—	20	—	13.8 ± 0.1	4.5 ± 0.1	1.4 ± 0.1	1.7 ± 0.1	55
8	10 ^b	20	—	17.3 ± 1.4	5.7 ± 0.6	2.1 ± 0.3	2.6 ± 0.3	60

Conversion and yields obtained by GC-FID analysis as average of two independent runs. Cyclic selectivity ratio (CR) obtained by dividing the combined yield of cyclic products by substrate conversion. ^a Amount formed in excess of the 10 mol% of **P1/P2/P3** used as additive. ^b **C3** used as catalyst instead of **C2**.

methylammonium salt—a known strong-binder of the R4OH-derived cavitands—resulted in a complete shutdown of the observed reactivity, demonstrating the crucial role of substrate encapsulation by **C2** in the reaction outcome. In the absence of acid co-catalyst neither nerol consumption nor product formation were observed (Table 2, entry 6), underscoring that the cavitand alone is insufficiently acidic to initiate the reaction. At 20 mol% loading of HCl in the absence of cavitand, the acidity in bulk solution was sufficient to activate the substrate providing some conversion, although indiscriminate reactivity was observed, and cyclic products were formed in a low ratio (Table 2, entry 7). Substitution of **C2** by the closed analogue **C3** lacking the phenol functionality (Fig. 2b) provided a similar

outcome (Table 2, entry 8). Taken together, these data underline the cooperative role of both catalysts and the necessity of a functional confined space for achieving selective cyclization of nerol.

We continued our optimization study exploring various reaction variables, including substrate concentration, catalyst and co-catalyst loadings, and stirring rate, while maintaining a consistent reaction time (Table 3). A maximum 59% conversion was obtained by increasing the HCl loading from 10 to 20 mol%, providing exclusive conversion to cyclic products with a significant and unprecedented bias towards limonene (Table 3, entry 2). Among the variables tested, increasing the co-catalyst (HCl) loading produced the most significant impact on reaction outcomes, with conversion rates and product for-

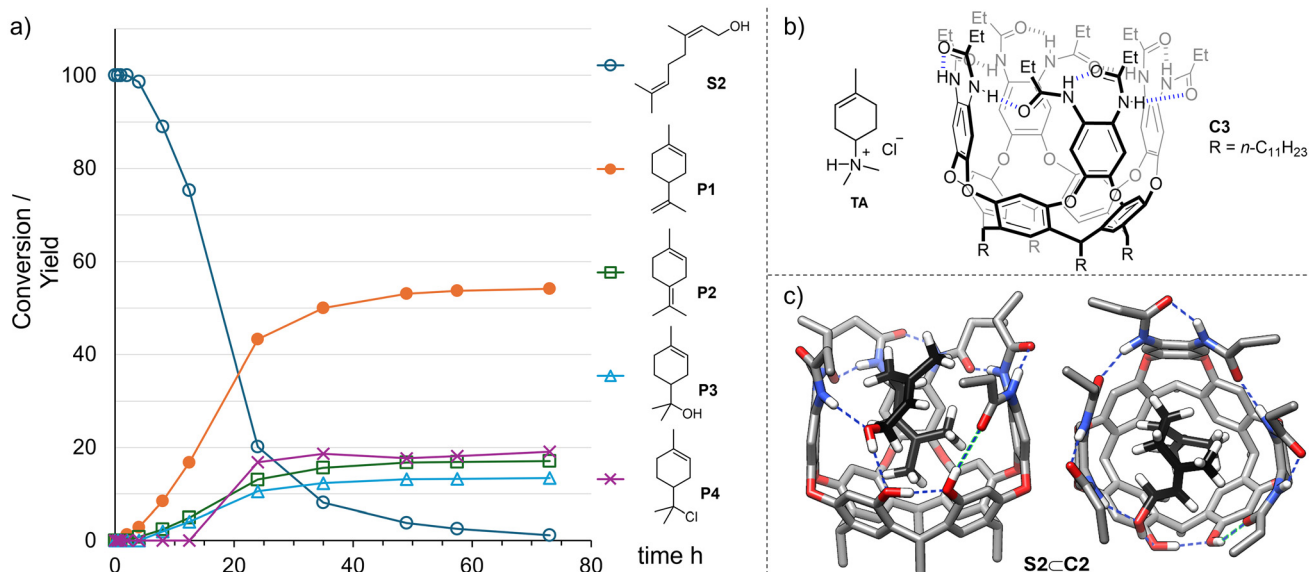
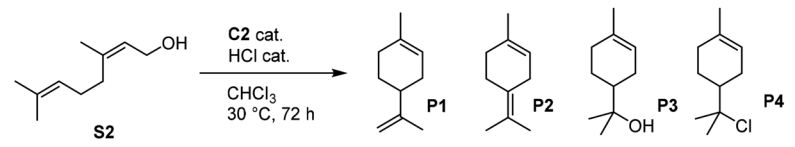


Fig. 2 (a) Reaction progress of the cyclization reaction of nerol (34 mM in CHCl₃, **C2** 10 mol%, aqueous HCl 30 mol%, 30 °C). Conversion is presented as the relative concentration of nerol with respect to initial concentration. (b) Schematic structures of the terpinyl cation analogues **TA** and the 4-walled reference cavitand **C3**. (c) DFT-optimized structure of **S2-C2** (side and top views). Nerol is depicted with a black carbon backbone, non-polar hydrogens of the cavitand omitted for clarity.



Table 3 Optimization of reaction conditions for the cyclization of nerol (**S2**) catalysed by **C2** and HCl (reaction time: 72 h)


Entry	S2 [mM]	Stirring rate [rpm]	C2 [mol%]	HCl [mol%]	Conv. [%]	Yield P1 [%]	Yield P2 [%]	Yield P3 [%]	Yield P4 [%]	CR [%]
1 ^a	100	550	10	10	23.4 ± 0.7	13.3 ± 0.5	4.5 ± 0.2	4.0 ± 0.1	—	93
2	100	550	10	20	59 ± 1	40 ± 6	12.4 ± 0.8	12 ± 1	—	>99
3	34	50	5	20	75 ± 5	40 ± 3	12.3 ± 0.8	8.0 ± 0.6	12.5 ± 0.9	97
4	34	50	10	20	73.4 ± 0.5	39.8 ± 0.1	12.4 ± 0.0	8.2 ± 0.1	11.9 ± 0.1	99
5	100	50	10	20	87 ± 1	43.7 ± 0.7	14.2 ± 0.2	11.1 ± 0.1	16.0 ± 0.0	98
6	100	50	—	20 ^b	5.6 ± 0.1	1.7 ± 0.2	0.5 ± 0.0	1.1 ± 0.3	—	59
7	34	550	5	30 ^b	96.9 ± 0.3	53.1 ± 0.0	16.4 ± 0.0	12.7 ± 0.0	19.2 ± 0.1	>99
8	34	550	10	30 ^b	99.3 ± 0.2	53.0 ± 0.2	17.0 ± 0.0	14.0 ± 0.3	19.6 ± 0.0	>99
9	100	50	5	20 ^b	96.8 ± 0.8	48 ± 1	15.6 ± 0.4	12.7 ± 0.2	17.7 ± 0.5	97
10	100	50	10	20 ^b	100 ± 0.0	49.4 ± 0.2	16.3 ± 0.1	13.4 ± 0.2	18.1 ± 0.1	97

Conversion and yields obtained by GC-FID analysis as average of two independent runs. Cyclic selectivity ratio (CR) obtained by dividing the combined yield of cyclic products by substrate conversion. ^a Table 1, entry 2. ^b Aqueous HCl was used.

mation rising markedly as co-catalyst levels increased. In comparison, increases in catalyst loading had a less pronounced effect, suggesting that the co-catalyst primarily facilitates the hydroxyl group activation step. This observation is in good alignment with terpene cyclizations catalysed by **C1**, where the cleavage of the leaving group has been identified as the rate-determining step. We also tested the effect of temperature by running the reaction at 45 °C instead of 30 °C (Table S2†). A significant increase in conversion was observed as expected, but the selectivity towards cyclic products decreased slightly, suggesting that the effect of the temperature was more pronounced on the non-catalysed background reaction.

An alternative explanation for the observed decay in reaction rate over time was loss of HCl by evaporation. When the reaction was carried out with gentle stirring (50 rpm instead of 550 rpm) the conversion increased (Table 3, entries 3–5), suggesting that evaporation of HCl may indeed be a significant factor for the reaction outcome. A maximum conversion of 87% was reached at 100 mM substrate concentration and 20 mol% loading of HCl. Under these conditions, an additional reaction product was observed, which we identified as α-terpinyl chloride (**P4**). At this point, we were intrigued by the slight but significant beneficial role of water (Table 2, entry 4), which we initially considered a potential source of reaction inhibition. We hypothesized whether aqueous HCl could be used directly in the cavitand-catalysed cyclization of nerol. In reactions catalysed by **C1**, accurate control of water content in the reaction mixture is crucial because the integrity of the hydrogen-bonded capsule is highly dependent on it. Conversely, the intramolecular hydrogen bond stabilization of self-folding cavitands make them more tolerant to adventitious water.^{33,34} Gratifyingly, when we subjected nerol to reaction using aqueous HCl as co-catalyst, total substrate conversion was observed (Table 3, entries 6–10, shaded). We postulate that the use of water as additive minimizes loss of HCl by evapor-

ation, leading to these improved conversion rates. Under these conditions, total selectivity towards cyclic products is observed, with limonene being formed in a remarkable 53% yield. The newfound reaction efficiency allows the reduction of **C2** loading to 5 mol% with minimal impact on the reaction performance. Additionally, cavitand **C2** can be easily recovered in pure form from the reaction mixture. Reaction progress analysis under the optimized conditions revealed that **P4** is formed in significant amounts only after 12 h, after most of **S2** is consumed, and it probably remained undetected in previous runs that proceeded at lower conversions (Fig. 2a). We hypothesize that **P4** is formed primarily from **P3** (α-terpineol) by an activation process akin to that proposed for **S2**, but occurring at a significantly lower reaction rate.

Mechanistic studies

Having established optimal conditions for the production of limonene with the **C2**/HCl catalytic system, we set out to rationalize the observed results on the basis of the molecular recognition properties of **C2**. Molecular modelling studies revealed that nerol presents a very good complementarity for **C2** owing to its contorted conformation, which allows the terminal isoprene group to fill the tapered end of the cavitand while the hydroxyl function is interacting through hydrogen bonding with the phenol groups and one of the amide NHs (Fig. 2c). We then set out to ascertain the binding affinities of the chemical species involved to justify the reaction turnover.† Using a ¹H NMR titration experiment, an association constant (*K*_a) of 8.8 M^{−1} was measured for the binding of nerol in **C2** (Fig. S4†). A value of *K*_a = 110 M^{−1} has been reported for

†Titrations were carried out by ¹H NMR in CDCl₃ without any added water. Attempts to carry out titration studies in the presence of water at concentrations similar to those in the catalysis experiments were unsuccessful due to broadening of the key resonances involved.



binding of nerol in **C1**, showcasing that very high substrate affinities are not a requirement for efficient supramolecular catalysis.³⁵ Additional titration experiments with compounds **P1–P4** revealed that the K_a 's of the reaction products are significantly below that of nerol, which explains the observed lack of inhibition by any of these species. Finally, we obtained a K_a of 298 M⁻¹ for terpinyl cation analogue **TA** (Fig. 2b), a known inhibitor of terpene cyclases,^{36,37} suggesting that the terpinyl cation remains in the cavity prior to elimination or trapping by nucleophiles. The binding of **TA** in **C2** was found to be in slow exchange regime relative to the NMR time scale at 238 K, allowing us to determine that **TA** is positioned with the dimethyl-amino group at the deepest section of the cavity (Fig. S7†). This observation suggests that upon cyclization of nerol in **C2**, the nascent terpinyl cation is positioned with the terminal methyl groups in close contact with the polar region defined by the phenol groups, facilitating the elimination reaction that leads to limonene.

To complete the mechanistic understanding of the reaction we carried out computational studies at the DFT level (Fig. 3). The optimized molecular models show that upon protonation of **S2C2** by HCl (intermediate **I1**), the protonated alcohol group of the substrate establishes cooperative hydrogen bonding with one phenol group and one amide carbonyl group on the cavitand's rim. At the same time, the chloride counterion is bound to the opposed phenol group and one carbonyl NH, providing a highly structured environment that is ripe for activation of the substrate. The cyclization to the terpinyl cation requires a barrier of only 12.2 kcal mol⁻¹ (**TS1**), much below the value of 24.5 kcal mol⁻¹ found for the reaction

mediated by HCl alone (Fig. S8†), corroborating the acceleration of the reaction under cooperative catalysis by **C2** and HCl. The transition state for the cyclization is S_N2-like, occurring with concerted cleavage and formation of the C–O and C–C bonds respectively. The terpinyl cation is obtained in a twist-boat conformation (**I2a**), and after relaxation to a half-chair conformation multiple orientations of the cation within the cavity are accessible. The extruded water molecule is hydrogen bonded to one of the phenol groups and one amide carbonyl group. Although experimental evidence of simultaneous binding of **TA** and water with **C2** could not be obtained,[‡] we carried out a titration experiment of **C2** with water that provides strong evidence for the proposed binding model (Fig. S5 and S6†). An arrangement of the terpinyl cation with one of the methyl groups in close contact with the extruded water was located (**I2b**, $d(\text{H–O}) = 1.59 \text{ \AA}$), from which facile elimination occurs leading to limonene (**I3**), confirming that substrate activation to yield the terpinyl cation is the rate determining step. Another orientation of the terpinyl cation was located with the tertiary C–H bond favourably oriented for elimination to terpinene (**I2c** → **T23** → **I4**, Fig. S9†), although at significantly longer distance from water ($d(\text{H–O}) = 2.64 \text{ \AA}$). Additionally, transition states leading to the formation of α -terpineol (**TS4**) and α -terpinyl chloride (**TS5**) were located, but we could not locate analogous minima leading to them (Fig. S9†). The low barrier calculated for the formation of limonene and the fact that the transition states leading to the minor products of the reaction are lower in energy suggest that the product selectivity is dictated by the diffusional rotation of the terpinyl cation within the cavity of **C2**.

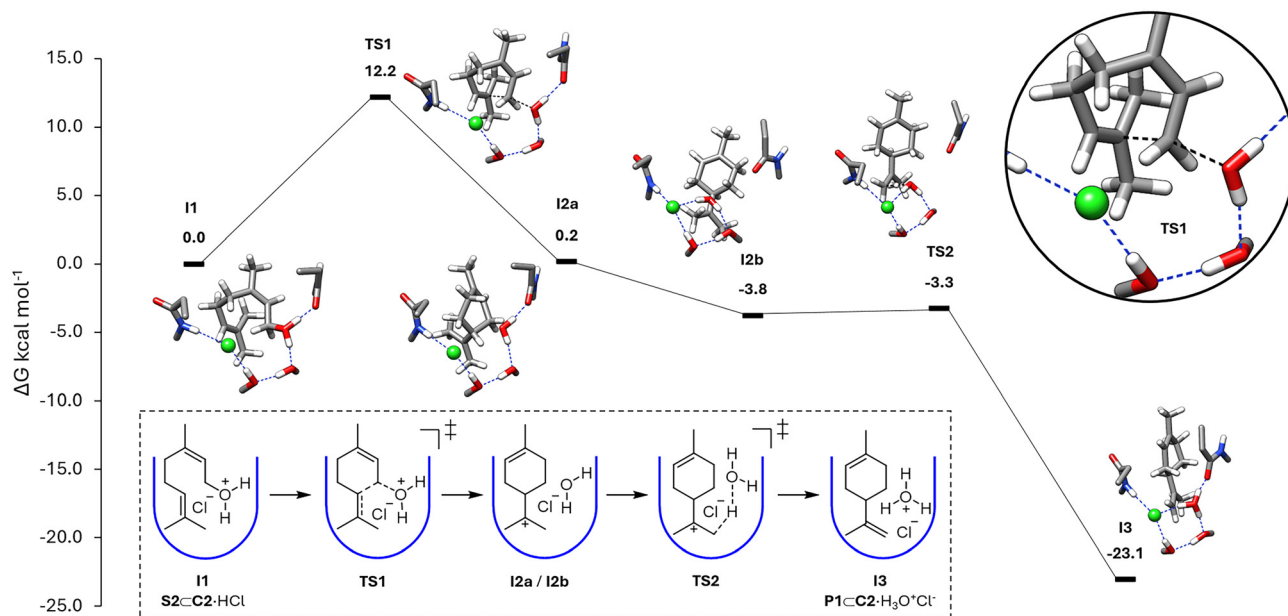


Fig. 3 Calculated reaction profile for the conversion of the nerol (**S2**) to limonene (**P2**) within **C2**, indicating relative Gibbs free energies (B3LYP/def2-SVP/GD3BJ// ω B97-X/def2-TZVPP).



Conclusions

We have developed an efficient terpene cyclization process of nerol catalysed by a partially bridged cavitand receptor **C2** and HCl. The reaction provides complete selectivity to cyclization products with a marked and unprecedented preference for limonene, reversing the selectivity pattern observed in reactions catalysed by the R4OH hexameric cage (**C1**). It is worth noting that products arising from 1,2- and 1,3-hydride shifts of the terpinyl cation (α - and γ -terpinene, isoterpinolene) as well as bicyclic eucalyptol are not formed in this process, but are consistently formed in reactions catalysed by **C1**. Catalysis by **C1** leads preferentially to the most thermodynamically stable cyclization compounds, while the precise molecular recognition of the terpinyl cation by **C2** makes it easier to obtain limonene, a product of kinetic control. The reaction operates at catalytic loadings as low as 5 mol%, and the catalyst can be easily recovered after use, features that bode well for potential synthetic applications of **C2**. This process relies on well-defined molecular recognition phenomena that provides substrate specificity, as opposed to the promiscuous reactivity observed with **C1**. The observed selectivity is reminiscent of the mode of action for natural monoterpene cyclases, where the intermediacy of linalyl pyrophosphate—a substrate preorganized for cyclization—is postulated.³⁸ The selectivity of the cyclization reaction is also driven by the molecular recognition of the key terpinyl cation intermediate within the confined space of **C2**. Titration experiments and computational studies at the DFT level explain the observed catalysis and acceleration, and provide clues about the origin of the product selectivity. Although production of limonene with simple small molecule catalysis is possible,³⁹ this work demonstrates that a functional pre-organized host of reduced symmetry is a viable alternative to **C1** for taming terpene cyclization processes. The use of cavitand receptors of expanded and flexible binding sites^{40–42} in combination with more sophisticated computational models that take into account the host dynamics appear as a promising avenue towards the development of rationally designed terpene cyclization processes of higher complexity.

Conflicts of interest

There are no conflicts to declare.

Data availability

The data that support the findings of this study are openly available in CORA.RDR at <https://doi.org/10.34810/data2113> (experimental data),⁴³ and in ioChem-BD at <https://doi.org/10.19061/iochem-bd-4-88> (computational data).⁴⁴

Acknowledgements

We are grateful for financial support from grants PID2020-113181GB-I00, PID2023-146498NB-I00, and REQ2021_B_05 funded by MICIU/AEI/10.13039/501100011033. We thank

AGAUR/Generalitat de Catalunya for funding (2021SGR623) and for a pre-doctoral fellowship to R. L. (2020 FI_B 00132). Open Access funding provided thanks to the CRUE-CSIC agreement with the RSC.

References

- 1 M. Morimoto, S. M. Bierschenk, K. T. Xia, R. G. Bergman, K. N. Raymond and F. D. Toste, Advances in supramolecular host-mediated reactivity, *Nat. Catal.*, 2020, **3**, 969–984.
- 2 B. Mitschke, M. Turberg and B. List, Confinement as a Unifying Element in Selective Catalysis, *Chem*, 2020, **6**, 2515–2532.
- 3 M. Raynal, P. Ballester, A. Vidal-Ferran and P. W. N. M. van Leeuwen, Supramolecular catalysis. Part 2: artificial enzyme mimics, *Chem. Soc. Rev.*, 2014, **43**, 1734–1787.
- 4 D. Ringe and G. A. Petsko, How Enzymes Work, *Science*, 2008, **320**, 1428–1429.
- 5 T. K. Piskorz, V. Martí-Centelles, R. L. Spicer, F. Duarte and P. J. Lusby, Picking the lock of coordination cage catalysis, *Chem. Sci.*, 2023, **14**, 11300–11331.
- 6 M. D. Ward, C. A. Hunter and N. H. Williams, Coordination Cages Based on Bis(pyrazolyl)pyridine Ligands: Structures, Dynamic Behavior, Guest Binding, and Catalysis, *Acc. Chem. Res.*, 2018, **51**, 2073–2082.
- 7 C. Gaeta, C. Talotta, M. De Rosa, P. La Manna, A. Soriente and P. Neri, The Hexameric Resorcinarene Capsule at Work: Supramolecular Catalysis in Confined Spaces, *Chem. – Eur. J.*, 2019, **25**, 4899–4913.
- 8 Q. Zhang, L. Catti and K. Tiefenbacher, Catalysis inside the Hexameric Resorcinarene Capsule, *Acc. Chem. Res.*, 2018, **51**, 2107–2114.
- 9 Q. Zhang and K. Tiefenbacher, Terpene cyclization catalysed inside a self-assembled cavity, *Nat. Chem.*, 2015, **7**, 197–202.
- 10 L.-D. Syntrivanis, I. Némethová, D. Schmid, S. Levi, A. Prescimone, F. Bissegger, D. T. Major and K. Tiefenbacher, Four-Step Access to the Sesquiterpene Natural Product Presilphiperfolan-1 β -ol and Unnatural Derivatives via Supramolecular Catalysis, *J. Am. Chem. Soc.*, 2020, **142**, 5894–5900.
- 11 E. Pahima, Q. Zhang, K. Tiefenbacher and D. T. Major, Discovering Monoterpene Catalysis Inside Nanocapsules with Multiscale Modeling and Experiments, *J. Am. Chem. Soc.*, 2019, **141**, 6234–6246.
- 12 T.-R. Li, C. Das, I. Cornu, A. Prescimone, G. Piccini and K. Tiefenbacher, Window[1]resorcin[3]arenes: A Novel Macrocyclic Able to Self-Assemble to a Catalytically Active Hexameric Cage, *JACS Au*, 2024, **4**, 1901–1910.
- 13 D. Sokolova, G. Piccini and K. Tiefenbacher, Enantioselective Tail-to-Head Terpene Cyclizations by Optically Active Hexameric Resorcin[4]arene Capsule Derivatives, *Angew. Chem., Int. Ed.*, 2022, **61**, e202203384.
- 14 D. Vidal, M. Costas and A. Lledó, A Deep Cavitand Receptor Functionalized with Fe(II) and Mn(II) Aminopyridine



- Complexes for Bioinspired Oxidation Catalysis, *ACS Catal.*, 2018, **8**, 3667–3672.
- 15 S. Korom and P. Ballester, Attachment of a RuII Complex to a Self-Folding Hexaamide Deep Cavitand, *J. Am. Chem. Soc.*, 2017, **139**, 12109–12112.
 - 16 F. R. Pinacho Crisóstomo, A. Lledó, S. R. Shenoy, T. Iwasawa and J. Rebek Jr., Recognition and Organocatalysis with a Synthetic Cavitand Receptor, *J. Am. Chem. Soc.*, 2009, **131**, 7402–7410.
 - 17 S. R. Shenoy, F. R. Pinacho Crisóstomo, T. Iwasawa and J. Rebek Jr., Organocatalysis In a Synthetic Receptor with an Inwardly Directed Carboxylic Acid, *J. Am. Chem. Soc.*, 2008, **130**, 5658–5659.
 - 18 S. Merget, L. Catti, G. Piccini and K. Tiefenbacher, Requirements for Terpene Cyclizations inside the Supramolecular Resorcinarene Capsule: Bound Water and Its Protonation Determine the Catalytic Activity, *J. Am. Chem. Soc.*, 2020, **142**, 4400–4410.
 - 19 A. Lledó and J. Rebek Jr., Self-folding cavitands: structural characterization of the induced-fit model, *Chem. Commun.*, 2010, **46**, 1637–1639.
 - 20 A. Lledó, R. J. Hooley and J. Rebek Jr., Recognition of Guests by Water-Stabilized Cavitand Hosts, *Org. Lett.*, 2008, **10**, 3669–3671.
 - 21 P. Ballester and M. A. Sarmentero, Hybrid Cavitand-Resorcin[4]arene Receptor for the Selective Binding of Choline and Related Compounds in Protic Media, *Org. Lett.*, 2006, **8**, 3477–3480.
 - 22 A. Lledó and A. Soler, Binding of ion pairs in a thiourea-functionalized self-folding cavitand, *Org. Chem. Front.*, 2017, **4**, 1244–1249.
 - 23 O. B. Berryman, A. C. Sather, A. Lledó and J. Rebek Jr., Switchable Catalysis with a Light-Responsive Cavitand, *Angew. Chem., Int. Ed.*, 2011, **50**, 9400–9403.
 - 24 F. Durola and J. Rebek Jr., The ouroborand: a cavitand with a coordination-driven switching device, *Angew. Chem., Int. Ed.*, 2010, **49**, 3189–3191.
 - 25 P. Restorp and J. Rebek Jr., Reaction of Isonitriles with Carboxylic Acids in a Cavitand: Observation of Elusive Isoimide Intermediates, *J. Am. Chem. Soc.*, 2008, **130**, 11850–11851.
 - 26 T. Iwasawa, P. Wash, C. Gibson and J. Rebek Jr., Reaction of an introverted carboxylic acid with carbodiimide, *Tetrahedron*, 2007, **63**, 6506–6511.
 - 27 T. Iwasawa, R. J. Hooley and J. Rebek Jr., Stabilization of labile carbonyl addition intermediates by a synthetic receptor, *Science*, 2007, **317**, 493–496.
 - 28 P. Amrhein, A. Shivanyuk, D. W. Johnson and J. Rebek Jr., Metal-Switching and Self-Inclusion of Functional Cavitands, *J. Am. Chem. Soc.*, 2002, **124**, 10349–10358.
 - 29 U. Luecking, J. Chen, D. M. Rudkevich and J. Rebek Jr., A Self-Folding Metallocavitand, *J. Am. Chem. Soc.*, 2001, **123**, 9929–9934.
 - 30 A. R. Renslo, F. C. Tucci, D. M. Rudkevich and J. Rebek, Synthesis and Assembly of Self-Complementary Cavitands, *J. Am. Chem. Soc.*, 2000, **122**, 4573–4582.
 - 31 A. R. Renslo and J. J. Rebek, Molecular Recognition with Introverted Functionality, *Angew. Chem., Int. Ed.*, 2000, **39**, 3281–3283.
 - 32 R. J. Hooley, T. Iwasawa and J. Rebek, Detection of Reactive Tetrahedral Intermediates in a Deep Cavitand with an Introverted Functionality, *J. Am. Chem. Soc.*, 2007, **129**, 15330–15339.
 - 33 A. Lledó and J. Rebek Jr., Deep cavitand receptors with pH-independent water solubility, *Chem. Commun.*, 2010, **46**, 8630–8632.
 - 34 T. Haino, D. M. Rudkevich, A. Shivanyuk, K. Rissanen and J. J. Rebek, Induced-Fit Molecular Recognition with Water-Soluble Cavitands, *Chem. – Eur. J.*, 2000, **6**, 3797–3805.
 - 35 T.-R. Li, C. Das, G. Piccini and K. Tiefenbacher, Tetrafluororesorcin[4]arene Hexameric Capsule Enables the Expansion of the Reactivity Space in Supramolecular Catalysis, *J. Am. Chem. Soc.*, 2025, **147**(13), 11108–11116.
 - 36 P. McGeady, H.-J. Pyun, R. M. Coates and R. Croteau, Biosynthesis of monoterpenes: Inhibition of (+)-pinene and (–)-pinene cyclases by thia and aza analogs of the 4R- and 4S- α -terpinyl carbocation, *Arch. Biochem. Biophys.*, 1992, **299**, 63–72.
 - 37 D. E. Cane, G. Yang, R. M. Coates, H. J. Pyun and T. M. Hohn, Trichodiene synthase. Synergistic inhibition by inorganic pyrophosphate and aza analogs of the bisabonyl cation, *J. Org. Chem.*, 1992, **57**, 3454–3462.
 - 38 B. R. Morehouse, R. P. Kumar, J. O. Matos, Q. Yu, A. Bannister, K. Malik, J. S. Temme, I. J. Krauss and D. D. Oprian, Direct Evidence of an Enzyme-Generated LPP Intermediate in (+)-Limonene Synthase Using a Fluorinated GPP Substrate Analog, *ACS Chem. Biol.*, 2019, **14**, 2035–2043.
 - 39 S. Tashiro, W. He, R. Hayashi, Y. Lin and M. Shionoya, Site-selective binding of terpenoids within a confined space of metal-macrocycle framework: substrate-specific promotion or inhibition of cyclization reactions, *Org. Chem. Front.*, 2021, **8**, 4071–4077.
 - 40 R. Álvarez-Yebra, R. López-Coll, N. Clos-Garrido, D. Lozano and A. Lledó, Calix[5]arene Self-Folding Cavitands: A New Family of Bio-Inspired Receptors with Enhanced Induced Fit Behavior, *Isr. J. Chem.*, 2024, **64**, e202300077.
 - 41 R. Álvarez-Yebra, R. López-Coll, P. Galán-Masferrer and A. Lledó, Enantioselective Molecular Recognition in a Flexible Self-Folding Cavitand, *Org. Lett.*, 2023, **25**, 3190–3194.
 - 42 D. Lozano, R. Álvarez-Yebra, R. López-Coll and A. Lledó, A flexible self-folding receptor for coronene, *Chem. Sci.*, 2019, **10**, 10351–10355.
 - 43 A. Lledó and R. López, *Replication data for: Terpene cyclization catalysis with a functional cavitand: driving selectivity through precise molecular recognition*, 2025, CORA.RDR, DOI: [10.34810/data2113](https://doi.org/10.34810/data2113).
 - 44 A. Lledó and R. López, *Hexaamidodiol catalysis*, 2025, ioChem-BD, DOI: [10.19061/iochem-bd-4-88](https://doi.org/10.19061/iochem-bd-4-88).

